SUPPORTING INFORMATION

The Influence of Fluorocarbon and Hydrocarbon Acyl Groups at the Surface of Bovine Carbonic Anhydrase II on the Kinetics of Denaturation by Sodium Dodecyl Sulfate

Andrew Lee, Katherine A. Mirica, and George M. Whitesides*

Department of Chemistry and Chemical Biology, Harvard University

12 Oxford St., Cambridge, MA, U.S.A.

*Author to who correspondence should be addressed:

E-mail: gwhitesides@gmwgroup.harvard.edu

ADDITIONAL BACKGROUND.

Discussion of the Properties of Fluorocarbon and Hydrocarbon Groups.

Molecular Surface Area (MSA). The surface areas of fluorocarbon groups are greater than those of hydrocarbon groups with the same carbon skeleton.[1] Computational modeling of the series of compounds X-H and X-$CONHCH_3$, where X = CF_3- or R_H-, shows that the MSA increases in the order CH_3- < CF_3- ~ CH_3CH_2- < $(CH_3)_2CH$- (Table 1 of the text).[2] CH_3CH_2- and $(CH_3)_2CH$ - groups are also anisotropic however, and do not have the same shape as the CF_3- group.[3] CF_3- groups are similar to $(CH_3)_2CH$- in steric bulk, as determined from the analysis of conformational equilibria of substituted cyclohexanes[4] and of the restricted rotation of substituted biphenyl systems.[3]

Hydrophobicity of Fluoroalkyl Surfactants. Surfactants with poly-fluorinated tails have approximately the same critical micellar concentration as surfactants with hydrocarbon tails with ~1.5 times more -CH_2- groups.[5-6] According to this metric for evaluating hydrophobicity, the hydrophobicity of the -CF_2- group lies between that of -CH_2- and -CH_2CH_2- groups, and is consistent with the idea that the hydrophobic interactions of alkyl and fluoroalkyl groups are determined predominantly by the surface area of these groups.

Weak Intermolecular Forces. Although fluorine has a greater number of electrons than hydrogen, the atomic polarizabilities of fluorine and hydrogen are similar; the ratio of polarizability to molecular volume, a dimensionless quantity, is lower for fluorine than hydrogen.[7] This comparison explains – according to Dunitz[7] – why the Van der Waals forces in fluorocarbon liquids are weaker than those in hydrocarbon liquids (in

which the molecules are similar in molecular volume). Values for the index of refraction for C_5F_{12} and C_5H_{12} (1.24 and 1.36, respectively) show the lower polarizability of fluorocarbons.[1] The weak attractive forces within fluorocarbon liquids are responsible for values of cohesive energy density and surface tension that are the lowest among organic liquids. Values for the surface tension of C_8F_{18} and C_8H_{18} (13.6 and 21.8 dyn cm^{-1}), correspond to excess surface free energies of 5.0 and 5.4 kcal mol^{-1} (conversion in units accounts for the surface areas of C_8F_{18} and C_8H_{18}).[8] These properties distinguish fluorocarbons from hydrocarbons in a way that is not related to molecular surface area. The low polarizability of fluorocarbon groups may be one reason why interactions with water molecules are poor, and perhaps poorer than those of hydrocarbon groups with water.

Values of the solubility parameter δ (the square root of the cohesive energy density) are lower for *n*-perfluoroalkanes than *n*-alkanes by ~ 20%.[9] Values of δ and molar volume predict the immiscibility of perfluorocarbons and hydrocarbon liquids of higher molecular weight; mixtures of *n*-perfluoroheptane and *n*-heptane phase-separate at 22 °C.[9-10] Fluorocarbon and hydrocarbon groups also phase-separate in mixtures of surfactants (e.g., perfluorooctanoate and SDS)[5,11] and in mixtures of polymers (e.g., poly(*N*-isopropyl-acrylamide) with $-CH_2C_7F_{15}$ or $-C_{18}H_{37}$ groups.[6] Phase separation gives the impression that fluorocarbons are "oleophobic", but is actually due to the unfavorable free energy of disrupting attractive forces among hydrocarbon groups in a pure sample (and those among fluorocarbon groups), and replacing them with the weaker attractive forces between hydrocarbon and fluorocarbon groups.

Fluorocarbon Groups in Protein Chemistry.

Increasing the Surface Area of Benzenesulfonamides with Fluorocarbon and Hydrocarbon "Tails". Analysis of the binding of BCA to benzenesulfonamide inhibitors provided an approach to investigating molecular recognition in proteins and its dependence on hydrophobic surface area.[12] The water-octanol partitioning of two series of inhibitors – *p*-$R_FCH_2NHCOC_6H_4SO_2NH_2$ ($R_F = F(CF_2)_n$-, n = 1 - 3) and *p*-R_H'$CH_2NHCOC_6H_4SO_2NH_2$ (R_H' = $H(CH_2)_n$-, n = 1 - 3) – showed agreement in the free energy of transfer per unit area (2.8 kcal mol^{-1} 100 $Å^{-2}$). Inhibitors with R_F- or R_H'-having similar molecular surface area (MSA) bound to BCA with similar affinity ($\Delta G°_B$; values were within 0.4 kcal mol^{-1}). The affinity of binding increased with MSA for both series, with a proportionality constant of 2.6 kcal mol^{-1} 100 $Å^{-2}$. These results supported the conclusion that the hydrophobic interactions of R_F- and R_H' of similar surface area with the "hydrophobic wall" of the binding cavity of BCA[13] are indistinguishable.

The importance of the -CH_2- spacer between R_F- and the amide group was, however, revealed in analysis of the binding affinity of inhibitors lacking a -CH_2- spacer, *p*-$R_FCONHCH_2C_6H_4SO_2NH_2$ ($R_F = F(CF_2)_n$-, n = 1 - 7). Binding was more favorable for these inhibitors, by ~ 1 kcal mol^{-1}, than binding of inhibitors with similar MSA in the series *p*-R_H'$CONHCH_2C_6H_4SO_2NH_2$ (R_H' = $H(CH_2)_n$-, n = 1 - 7). This result suggested that R_F- groups can also affect molecular recognition in these experiments through inductive effects. In this instance, the R_F- groups would, we presume, increase the strength of hydrogen-bonds between the N-H donor of the inhibitor and the binding pocket of BCA.

Substitution of CH_3- groups with CF_3- groups in Helical Peptides.

Polypeptides that fold into oligomeric, helical domains with a hydrophobic core have provided a way to analyze the effect of fluorocarbon groups on protein folding. Bilgiçer et al. designed a peptide containing four trifluoroleucine and three trifluorovaline residues (within a sequence of 33 amino acid residues) to fold into an α-helix and direct CF_3- groups to one face of the helix.[14] Coiled-coils assembled from these peptides were more stable than those assembled from a control peptide (sequences with Leu and Val) towards thermal denaturation (T_m = 62 °C compared to 47 °C), and towards denaturation by guanidinium hydrochloride (Gdn-HCl; by ~0.07 kcal mol^{-1} per CF_3- group).

Marsh et al. found that substitution of eight Leu with hexafluoroleucine residues in the hydrophobic core of a four-helix bundle increased the stability towards denaturation by Gdn-HCl.[15] The increase in stability (0.3 kcal mol^{-1} per hexafluoroleucine residue) was consistent with the demonstration that hexafluoroleucine is more hydrophobic than Leu in water-octanol partitioning (by 0.4 kcal mol^{-1}). This agreement led to the conclusion that the hydrophobicity of CF_3- groups, and not oleophobicity or a "fluorous effect", was responsible for the stabilization of quaternary structure.

The influence of CF_3- is not limited to space-filling effects. How do CF_3- groups stabilize the assembly of helical peptides? Are hydrophobic interactions, determined by non-polar surface area, the only responsible factor? Koksch et al., addressed this issue by analyzing helical peptides containing the non-native amino acid residue 2-amino-4,4,4-trifluorobutanoic acid (Tfe-Gly). Tfe-Gly was selected for its ability to mimic the space-filling properties of Leu.[16] Coiled-coils assembled from

peptides with Tfe-Gly were less stable than those with Leu (T_m = 59 and 74 °C, respectively). This system suggested that CF_3- groups are distinguishable from isopropyl groups, and that CF_3- groups participate in more than just hydrophobic interactions. Thus, Tfe-Gly destabilized the coiled-coils as a result of what was interpreted to be the introduction of C-F dipoles within the hydrophobic core.[17]

Studies reporting the influence of fluorocarbon groups in globular proteins do not reach a consensus; the influence of fluorine on the stability of the folded protein depends on the position of substitution. Substitution with a single trifluorovaline residue increased the stability of a 56-residue α,β protein (NTL9) towards denaturation in Gdn-HCl by 1.4 kcal mol^{-1}, an effect greater than that observed in helical peptides (≤ 0.2 kcal mol^{-1} per CF_3- group).[18] The objective of Woll et al., by substituting 5-fluorophenylalanine (F_5-Phe) into a 35-residue subdomain (from chicken villin headpiece), was to induce both quadrupolar interactions and hydrophobic interactions.[19] The results of substitution depended on the site of F_5-Phe, ranging from stabilization of folded protein by 0.6 kcal mol^{-1} to destabilization of the protein by 0.8 kcal mol^{-1}.

SUPPLEMENTAL RESULTS AND DISCUSSION.

Figure S1. Survey of reagents for trifluoroacetylation of Lys-ε-NH_3^+ groups of BCA. Reaction mixtures were prepared by adding acylating agent (amounts, in number of stoichiometric equivalents with respect to lysine residues, given to the right) dissolved in acetonitrile or dioxane to buffered solutions of BCA (20 μM in protein, pH = 9.0 with 0.1 M HEPBS). Reaction mixtures were analyzed by CE in bare, fused silica capillaries filled with tris-glycine buffer (pH = 8.3; [glycine] = 192 mM, [tris] = 25 mM). Traces in Figure S1 are labeled with the trifluoroacetylating agent used in the reaction to the right of the trace. Traces were collected using capillaries with a total length 60 cm and length of 50 cm to the detector.

Figure S1.

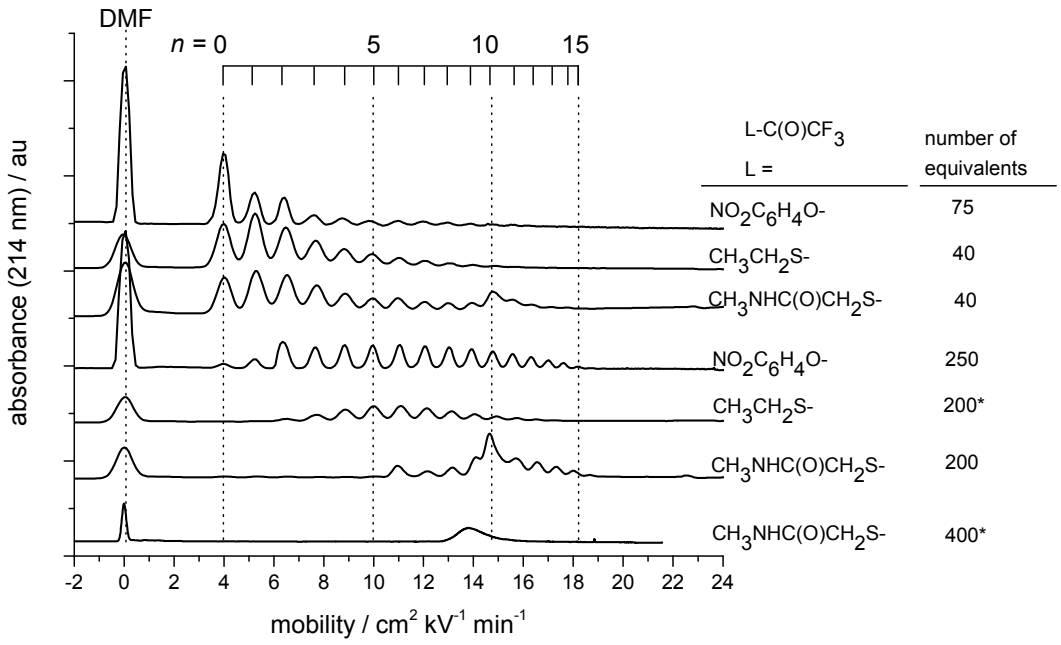

Figure S2. Denaturation of **(A)** BCA-[CF_3CONH-]$_n$ and **(B)** BCA-[CH_3CONH-]$_n$ in 3.0 mM SDS. Aliquots from reaction mixtures were analyzed by CE (30 kV) using capillaries (107 cm in length, 100 cm between inlet and detector) filled with Tris-Gly buffer and 3.0 mM SDS. To serve as an internal standard and report on the electro-osmotic flow, DMF (1 mM) was added to the aliquots prior to injection. Absorbance at 214 nm detected derivatives of BCA in the folded state and in complexes with SDS. Prior to the addition of SDS, charge ladders were analyzed by CE in running buffer without SDS (electropherograms at the bottom of each set, labeled with a time points of 0.0 hrs). Mobilities were slightly higher in buffer without SDS than in buffer with 3.0 mM SDS. The shift to lower values of mobility in solutions of SDS was consistent with screening of the charge of proteins by SDS; addition of 3.0 mM SDS increased the ionic strength of the buffer from ~8.3 to ~11.3 mM.

Figure S2.

(A)

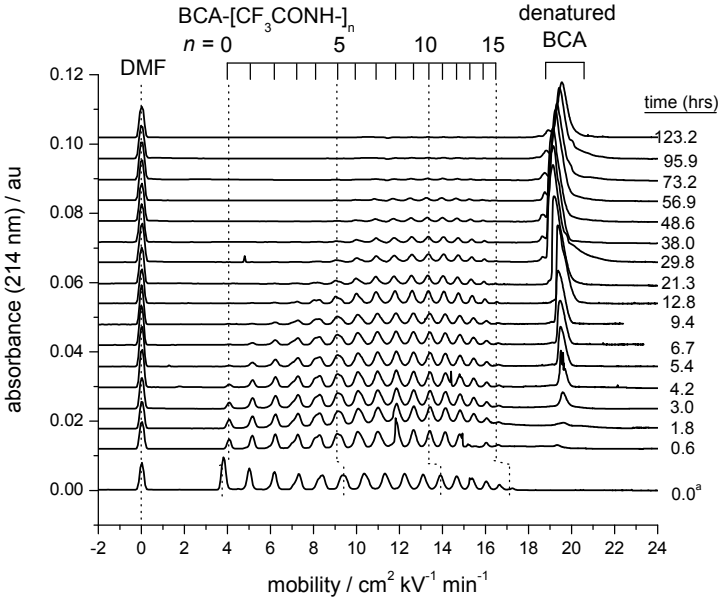
BCA-[CF3CONH-]n
n = 0
5
10
15
denatured
BCA
DMF
time (hrs)
123.2
95.9
73.2
56.9
48.6
38.0
29.8
21.3
12.8
9.4
6.7
5.4
4.2
3.0
1.8
0.6
0.0a
absorbance (214 nm) / au
mobility / cm2 kV-1 min-1

(B)

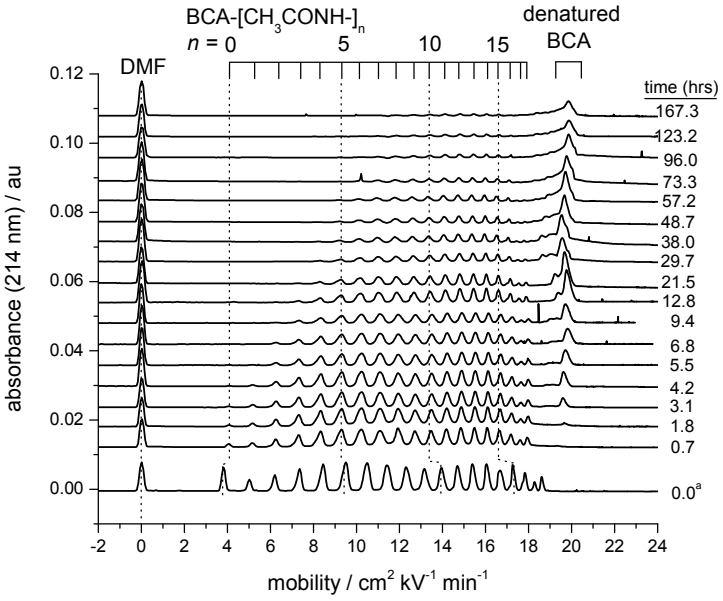
BCA-[CH3CONH-]n
n = 0
5
10
15
denatured
BCA
DMF
time (hrs)
167.3
123.2
96.0
73.3
57.2
48.7
38.0
29.7
21.5
12.8
9.4
6.8
5.5
4.2
3.1
1.8
0.7
0.0a
absorbance (214 nm) / au
mobility / cm2 kV-1 min-1

Figure S3. Denaturation of **(A)** BCA-[CF_3CONH-]$_n$ and **(B)** BCA-[CH_3CH_2CONH-]$_n$ in 3.0 mM SDS. Aliquots from reaction mixtures were analyzed by CE (30 kV) using capillaries (107 cm in length, 100 cm between inlet and detector) filled with Tris-Gly buffer and 3.0 mM SDS. To serve as an internal standard and report on the electro-osmotic flow, DMF (1 mM) was added to the aliquots prior to injection. Absorbance at 214 nm detected derivatives of BCA in the folded state and in complexes with SDS. Prior to the addition of SDS, charge ladders were analyzed by CE in running buffer without SDS (electropherograms at the bottom of each set, labeled with a time points of 0.0 hrs). Mobilities were slightly higher in buffer without SDS than in buffer with 3.0 mM SDS. The shift to lower values of mobility in solutions of SDS was consistent with screening of the charge of proteins by SDS; addition of 3.0 mM SDS increased the ionic strength of the buffer from ~8.3 to ~11.3 mM.

Figure S3.

(A)

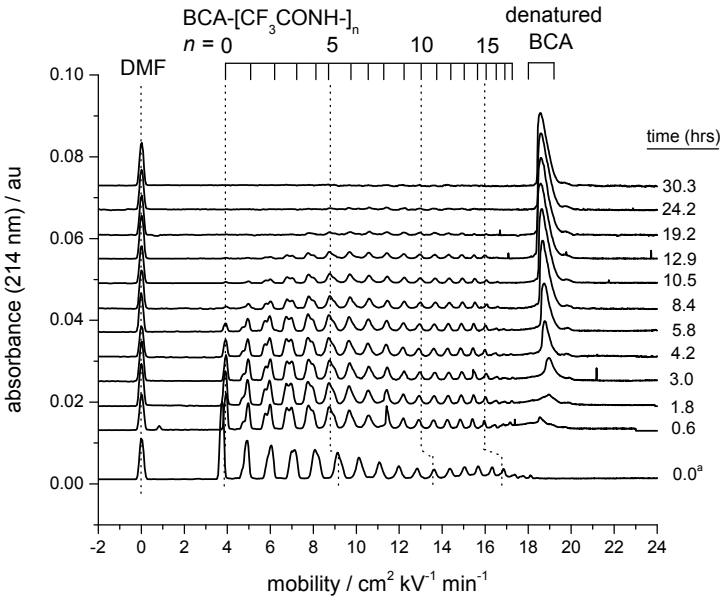
BCA-[CF3CONH-]n
n = 0
5
10
15
denatured
BCA
DMF
time (hrs)
30.3
24.2
19.2
12.9
10.5
8.4
5.8
4.2
3.0
1.8
0.6
0.0a
absorbance (214 nm) / au
mobility / cm2 kV-1 min-1

(B)

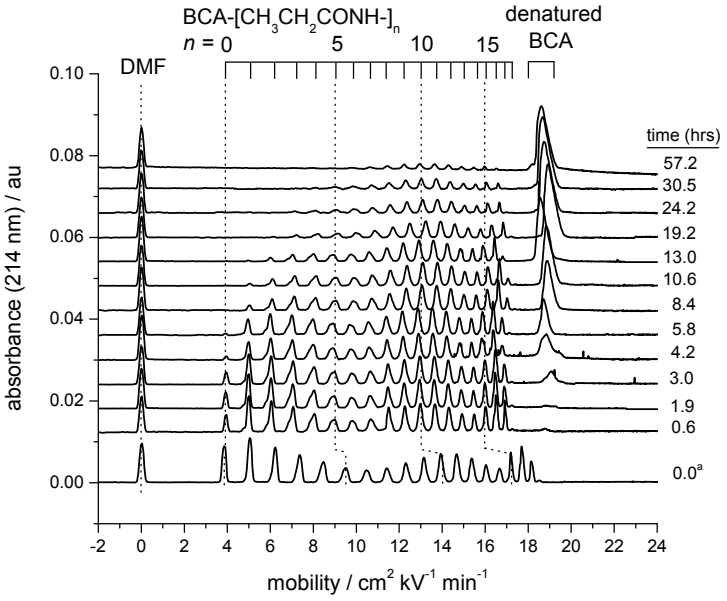
BCA-[CH3CH2CONH-]n
n = 0
5
10
15
denatured
BCA
DMF
time (hrs)
57.2
30.5
24.2
19.2
13.0
10.6
8.4
5.8
4.2
3.0
1.9
0.6
0.0a
absorbance (214 nm) / au
mobility / cm2 kV-1 min-1

Figure S4. Rates of Denaturation of Determined by the Decrease in Areas of Peaks for Folded Protein. Points show the amount of folded protein in rungs for **(A)** BCA-[CH_3CONH-]$_n$ and **(B)** BCA-[CH_3CH_2CONH-]$_n$, determined from areas of peaks observed in CE; the amount of folded protein is expressed as a fraction of the initial amount of folded protein (i.e., prior to the addition of SDS). Plots show data for n = 1, 4, 7, 10, and 13 for visual clarity. Data are from one of four repetitions of the experiment; we do not show experimental uncertainties because the times at which reaction mixtures were analyzed varied across repetitions. Lines fitting the points represent single-exponential decay, and were obtained by fitting the equation $2.3RT\log\left(A_t A_0^{-1}\right) = -k \cdot t$, where A_t and A_0 are the areas of peaks at times t and zero hours after the addition of SDS; k is the pseudo-first-order rate constant (R is the Boltzmann constant and T is the temperature).

Figure S4.

A)

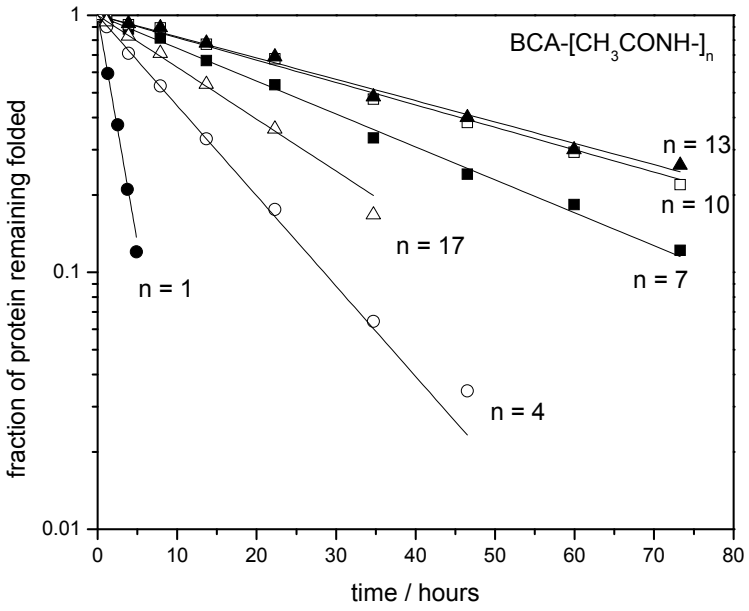
BCA-[CH3CONH-]n
n = 13
n = 10
n = 17
n = 7
n = 1
n = 4
fraction of protein remaining folded
time / hours
1
0.1
0.01
0
10
20
30
40
50
60
70
80

B)

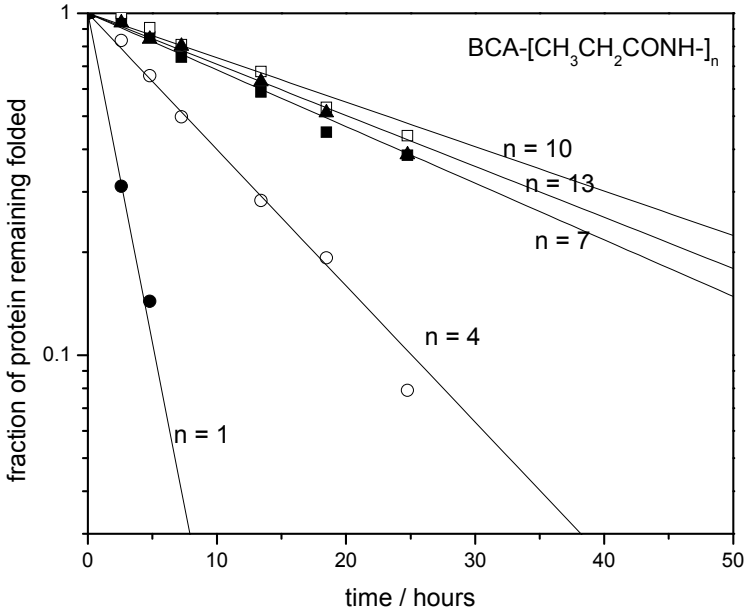
BCA-[CH3CH2CONH-]n
n = 10
n = 13
n = 7
n = 4
n = 1
fraction of protein remaining folded
time / hours
1
0.1
0
10
20
30
40
50

Analytical Method for Fitting Kinetics of Denaturation.

Analytical Model for $k_{Ac,n}$. We developed a model for $k_{Ac,n}$ as a function of n, with two objectives: (i) to interpret the curves for $k_{Ac,n}$ as results of the effect of acylation on electrostatic and hydrophobic interactions; (ii) to rationalize why the $k_{Ac,n}$ is relatively insensitive to n in the range $7 < n < 14$, and thus why values of $\Delta G^{\mp}_{R_H} - \Delta G^{\mp}_{CF_3}$ are approximately constant in this range. We hypothesized that the curves for $k_{Ac,n}$ are the result of contributions from competing mechanisms for denaturation. We analyzed the data in Figure 5 of the text with a model in which $k_{Ac,n}$ is determined by $k_{1,n}$ and $k_{2,n}$ (Eq. S1). In this model, $k_{1,n}$ and $k_{2,n}$ are the rates for competing mechanisms of denaturation; both $k_{1,n}$ and $k_{2,n}$ are influenced by the acylation of BCA. Equations S2 and S3 show that $k_{1,n}$ and $k_{2,n}$ depend on the number of acylations (n), the contribution of each acylation to the free energy of activation ($\Delta\Delta G_1^{\mp}$ and $\Delta\Delta G_2^{\mp}$), and rates for the denaturation of unacylated BCA through each mechanism ($k_{1,0}$ and $k_{2,0}$). Equation S4 is derived by substitution of the expressions in S2 and S3 into Eq. S1.

$$k_{Ac,n} = k_{1,n} + k_{2,n} \tag{S1}$$

$$k_{1,n} = k_{1,0} \cdot 10^{\frac{-\Delta\Delta G_1^{\mp} \cdot n}{2.3RT}} \tag{S2}$$

$$k_{2,n} = k_{2,0} \cdot 10^{\frac{-\Delta\Delta G_2^{\mp} \cdot n}{2.3RT}} \tag{S3}$$

$$\log k_{Ac,n} = \log\left(k_{1,0} \cdot 10^{\frac{-\Delta\Delta G_1^{\mp} \cdot n}{2.3RT}} + k_{2,0} \cdot 10^{\frac{-\Delta\Delta G_2^{\mp} \cdot n}{2.3RT}} \right) \tag{S4}$$

The solid curves in the plots of Figure 5 are the least-squares fit of Eq. S4 to the points in the range $0 \leq n \leq 14$. In the fitting procedure, the parameters $k_{1,0}$, $k_{2,0}$, $\Delta\Delta G_1^{\mp}$ and $\Delta\Delta G_2^{\mp}$ are allowed to vary; $k_{1,0}$ and $k_{2,0}$ are constrained to the same value in separate sets of data, because they describe the denaturation of unacylated BCA (the same protein in each set of data).[20] We fit the model to the selection of data with $0 \leq n \leq 14$, because this range corresponds to the data available for BCA-[CF_3CONH-]$_n$ and $\Delta G_{R_H}^{\mp} - \Delta G_{CF_3}^{\mp}$ in Figure 6 of the text. Points with $n \geq 15$ were not included in the fit; the increase in rate in this range implicated a factor separate from those responsible for the kinetics in the range $0 \leq n \leq 14$. Analysis of the full range of the data, using a model with an additional term ($k_{3,n}$) to address the points with $n \geq 15$, also gave a reasonable fit (results shown in Fig. S5).

We settled on the model in Eq. S4, after testing the fit of several other models, because of its simplicity and ability to reproduce the key features of the data: (i) the decrease in $k_{\mathrm{Ac},n}$ at low numbers of acylation; (ii) relatively constant values of $k_{\mathrm{Ac},n}$ at moderate numbers of acylations. The curves for $k_{\mathrm{Ac},n}$ generated by the model were compatible with the data for $\Delta G_{R_H}^{\mp} - \Delta G_{CF_3}^{\mp}$ in Figure 6 of the text, and demonstrated that the model distinguishes the results for BCA-[CF_3CONH-]$_n$ and BCA-[R_HCONH-]$_n$ reasonably well; the agreement between the results and the prediction of $\Delta G_{R_H}^{\mp} - \Delta G_{CF_3}^{\mp}$ (from the curves determined by Eq. S4) is shown in Fig. S6.

Interpretation of $k_{\mathrm{Ac},n}$ with this model suggests a change in the mechanism of denaturation as the extent of modification to the surface of BCA increases. The decrease in $k_{\mathrm{Ac},n}$ at low numbers of acylations is determined by $k_{1,n}$ (dashed line in Figure 5). At moderate numbers of acylations, the contribution of $k_{1,n}$ decreases while the contribution

Figure S5. Model with Three Contributions for the Kinetics of Denaturation of BCA-[CF_3CONH-]$_n$ and BCA-[R_HCONH-]$_n$. Values of $k_{Ac,n}$ are the same as those in Figure 5 in the text. Curved lines were obtained by the fit of log $k_{Ac,n}$ = log [$k_1(n) + k_2(n) + k_3(n)$] to the points, with the adjustable parameters $k_{1,0}$, $k_{2,0}$, $k_{3,0}$, $\Delta\Delta G_1^{\mp}$, $\Delta\Delta G_2^{\mp}$, and $\Delta\Delta G_3^{\mp}$. The slope of the lines for log k_n represent the quantity $\Delta\Delta G_1^{\mp} / 2.3RT$ and are unitless.

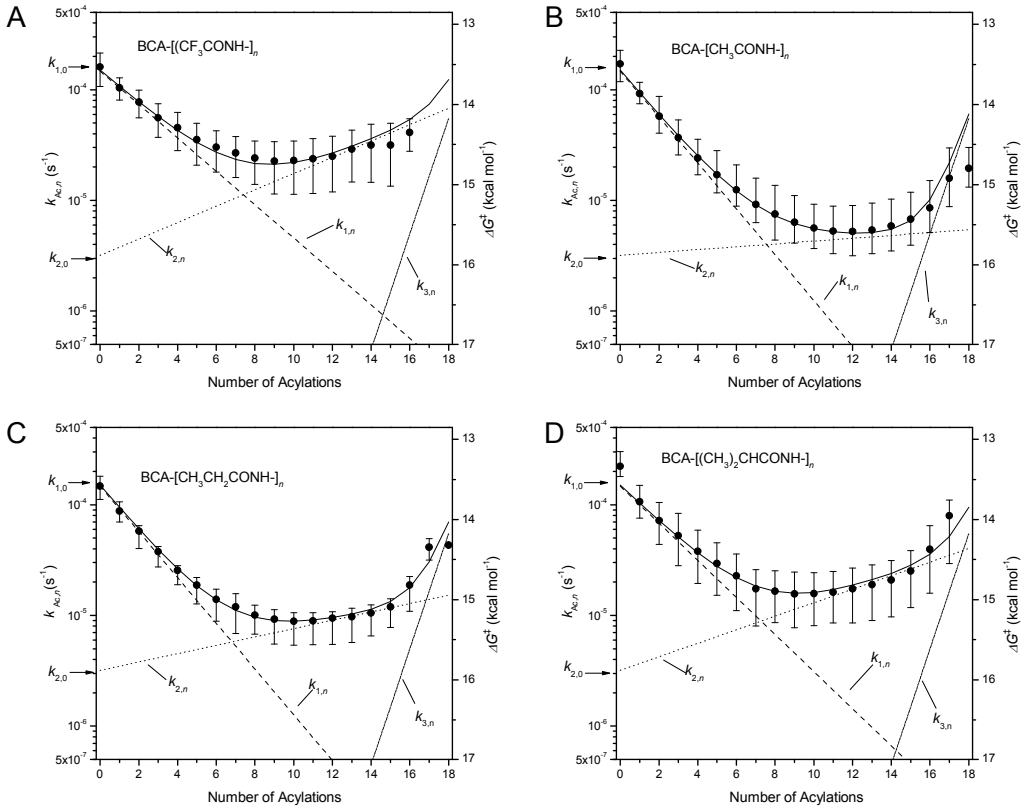

Figure S6. Prediction of $\Delta G^{\mp}_{R_H} - \Delta G^{\mp}_{CF_3}$ from models for $k_{\mathrm{Ac},n}$. Curves fitting data for $k_{\mathrm{Ac},n}$, determined from the model described in Equations S1-S4, were used to calculated values of $\Delta G^{\mp}_{R_H} - \Delta G^{\mp}_{CF_3}$ used to compare the denaturation of BCA-[CF_3CONH-]$_n$ with (A) BCA-[CH_3CONH-]$_n$; (B) BCA-[CH_3CH_2CONH-]$_n$; (C) BCA-[$(CH_3)_2CHCONH$-]$_n$.

Figure S6.

(A) BCA-[CH_3CONH]- vs BCA-[CF_3CONH]-

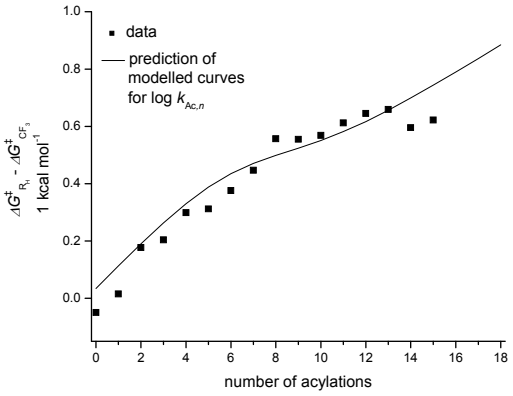

(B) BCA-[CH_3CH_2CONH]- vs BCA-[CF_3CONH]-

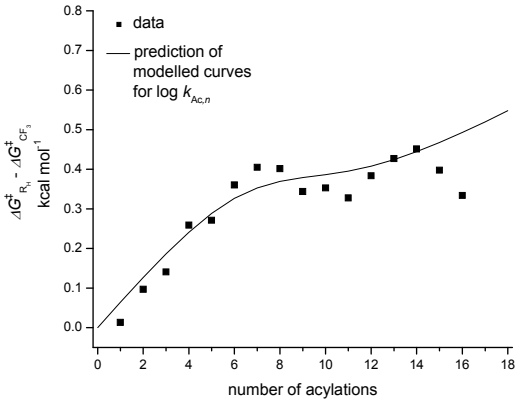

(C) BCA-[$(CH_3)_2CHCONH$]- vs BCA-[CF_3CONH]-

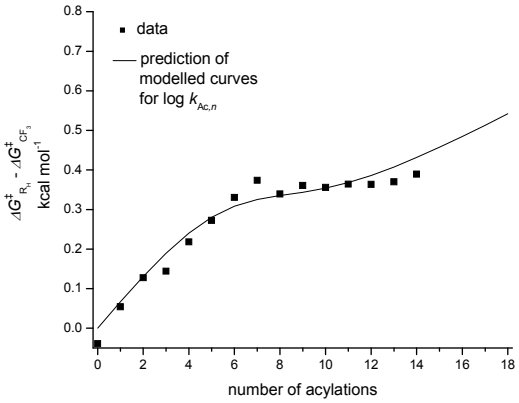

of $k_{2,n}$ to $k_{Ac,n}$ increases (dotted line in Figure 5). Values of $k_{Ac,n}$ do not change much in this range for two reasons: (i) when $k_{Ac,n}$ depends on both $k_{1,n}$ and $k_{2,n}$ ($n \sim 7$ - 10) the decrease in $k_{1,n}$ is compensated by an increase in $k_{2,n}$; (ii) $k_{2,n}$ is not considerably sensitive to n (or is insensitive to n, in the case of BCA-[CH_3CONH-]$_n$).

Interpretation of $k_{1,n}$: Opposing Contributions from Electrostatic and Hydrophobic Interactions. For each charge ladder, rates of denaturation ($k_{Ac,n}$) decreased with n at low numbers of acylations. The decrease in rate is compatible with unfavorable electrostatic interactions between negatively charged SDS molecules and proteins with increasing amounts of net negative charge. This observation supports the hypothesis that the rate-limiting step in $k_{1,n}$ involves the association of SDS with the protein. We interpret the differences in $k_{1,n}$ between BCA-[CF_3CONH-]$_n$ and BCA-[R_HCONH-]$_n$ as the result of hydrophobic interactions of CF_3CONH- and R_HCONH- with SDS. The slopes of the lines for log $k_{1,n}$ (Figure 5) suggest an order in hydrophobicity of CH_3CONH- < CH_3CH_2CONH- < $(CH_3)_2CHCONH$- < CF_3CONH-. According to this interpretation of $k_{1,n}$, hydrophobic interactions between SDS and acyl groups at the surface of derivatives of BCA are favorable for the association of SDS and lead to an increase in the rate of denaturation. These interactions partially compensate for unfavorable electrostatic interactions and result in rates of denaturation that are characteristic of the hydrophobicity of CF_3CONH- and R_HCONH- groups.

Interpretation of $k_{2,n}$. The contribution of $k_{2,n}$ is responsible for values of $k_{Ac,n}$ that are somewhat insensitive to n at moderate numbers of acylations. We do not propose an underlying mechanism for $k_{2,n}$; we can only say that it is less sensitive to the acylation of Lys-ε-NH_3^+ groups than the mechanism responsible for $k_{1,n}$ (the slopes of the lines for

log $k_{2,n}$ show that acylation contributes < 0.1 kcal mol^{-1} per group to the free energy of activation). The lines for log $k_{2,n}$ however show a dependence on the choice of acyl group – values of slope increase in the order CH_3CONH- < CH_3CH_2CONH- < $(CH_3)_2CHCONH$- < CF_3CONH- – and show that hydrophobic interactions of the acyl groups are also involved in the mechanism of denaturation of derivatives with $7 \leq n \leq 14$.

EXPERIMENTAL SECTION.

Sources of Chemicals and Reagents. All chemicals were reagent grade unless stated otherwise. Samples of SDS, Tris-Gly buffer, and Bovine Carbonic Anydrase II were purchased from Sigma-Aldrich (St. Louis, MO). SDS was purified by crystallization from hot ethanol twice, dried under vacuum, and used without further characterization. Dialysis cassettes (1.0 mL volume, 10-kDa molecular weight cutoff) were purchased from Pierce Biochemical.

Compounds for Water-Octanol Partitioning: $C_6H_5CH_2$-NH-C(O)R. *N*-benzylacetamide was obtained from Sigma-Aldrich ((St. Louis, MO). We prepared the compounds *N*-benzyltrifluoroacetamide, *N*-benzylpropanamide, *N*-benzyl-2-methylpropanamide, *N*-benzylhexanamide by reaction of benzylamine with selected acylating agents (i.e. trifluoroacetic anhydride, propionic anhydride, isobutyric anhydride, and hexanoyl chloride); we followed the procedure reported by Barluenga et. al..[21] We briefly describe the synthetic procedure. We added two equivalents of acylating agent dropwise to a solution of benzylamine (~0.5 M) in dichloromethane and pyridine (10% by volume) that was cooled by an ice bath. After stirring for 5 min., the mixture was brought to room temperature and stirred for 1 hour; water was added to

quench the reaction. The organic layer was removed, concentrated, and purified either by silica gel chromatography (in the case of *N*-benzylpropanamide) or by re-crystallization from mixtures of methanol and water (*N*-benzyltrifluoroacetamide, *N*-benzyl-2-methylpropanamide, *N*-benzylhexanamide). Compounds were characterized, and the purity of samples (>95%) was estimated by ^{1}H NMR.

Measurement of Water-Octanol Partitioning Coefficients. We measured the water-octanol partitioning coefficients for each $C_6H_5CH_2$-NH-C(O)R listed in the previous section by measuring the concentrations of $C_6H_5CH_2$-NH-C(O)R in the 1-octanol-rich fraction and the aqueous-rich fraction of emulsions consisting of equal volumes of 1-octanol and aqueous buffer (0.01 M sodium phosphate, pH = 7.4). Aliquots (300 μLs) of stock solutions of $C_6H_5CH_2$-NH-C(O)R in 1-octanol (100 mgs per mL) were added to aliquots of aqueous buffer (300 μLs) in glass vials. After the emulsion was vigorously stirred at 22 °C for 24 hours, it was separated by centrifugation. Concentrations of $C_6H_5CH_2$-NH-C(O)R in the 1-octanol-rich fraction and the aqueous-rich fraction were determined by diluting aliquots taken from these fractions and measuring the absorbance at 257 nm. The water-octanol partitioning coefficient was determined by calculating the ratio of the absorbance in the 1-octanol-rich fraction to the absorbance in the aqueous-rich fraction (after correcting for dilution).

Quantitative Analysis of Peak Areas in Capillary Electrophoresis. Quantitative analysis of peaks in CE allowed us to determine the rates of denaturation for BCA-[CF_3CONH-]$_n$ and BCA-[R_HCONH-]$_n$. Areas of peaks for folded protein decreased over time for two reasons: i) denaturation by SDS; ii) a decrease in overall concentration of protein in the reaction mixture (~ 10% over the course of 72 hours), due to either

dilution during dialysis or leakage of protein from the dialysis cassette. We multiplied peak areas obtained by CE with a correction factor, ($[BCA](t)\ [BCA]_0^{-1}$), to account for the decrease in overall protein concentration, where $[BCA]_0$ and $[BCA](t)$ are the initial concentration and concentration at time t after the addition of SDS (measured by UV absorbance; $\varepsilon_{280} = 57{,}000\ M^{-1}\ cm^{-1}$). We assumed that all forms of BCA were diluted equivalently. In addition, we multiplied peak areas by a factor ($L \cdot \tau^{-1}$; L is the distance from the inlet to the detetctor, τ is the retention time) to correct for differences in residence time in front of the UV detector. The amount of protein that remains folded at time t after the addition of SDS, expressed as the fraction of the initial amount of protein, was obtained from the quantity ($A(t)\ A_0^{-1}$), where $A(t)$ and A_0 are the corrected areas of peaks.

Denaturation of Charge Ladders of BCA. We used the same protocol used by Gudiksen.[22] Briefly, a solution of Tris-Gly buffer (1.0 L) was prepared from a stock solution of concentrated Tris-Gly (10-fold concentrated) and a stock solution of SDS in water (20.0 mM), and allowed to stir at 22 °C for 8 hours. Samples of charge ladders of BCA (60 μM in Tris-Gly buffer) were added to dialysis cassettes and placed into a bath of a buffered solution of 3.0 mM SDS, to begin the addition of SDS and the denaturation reaction.

REFERENCES.

(1) Smart, B. E. *J. Fluorine Chem.* **2001**, *109*, 3-11.
(2) Values of MSA were calculated using the software program MOE, developed by the Chemical Computing Group (Montreal, Canada).
(3) Leroux, F. *ChemBioChem* **2004**, *5*, 644-649.
(4) Uneyama, K. *Organofluorine Chemistry*; Blackwell Publishing, Ltd.: Oxford, UK, 2006.

(5) Nordstierna, L.; Furo, I.; Stilbs, P. *J. Am. Chem. Soc.* **2006**, *128*, 6704-6712.
(6) Kujawa, P.; Raju, B. B.; Winnik, F. M. *Langmuir* **2005**, *21*, 10046-10053.
(7) Dunitz, J. D. *ChemBioChem* **2004**, *5*, 614-621.
(8) Quantities in units of kcal mol^{-1} represent the energy required to increase the area of the liquid-air interface by an amount corresponding to 1 mol of material. Values were calculated using data for surface tension and molecular surface area, estimated from the molecular weight and density of the liquids at 22 °C.
(9) Hildebrand, J. H. *Regular and related solutions; the solubility of gases, liquids, and solids*; Van Nostrand Reinhhold Co.: New York, 1970.
(10) Barthel-Rosa, L. P.; Gladysz, J. A. *Coord. Chem. Rev.* **1999**, *192*, 587-605.
(11) Nakano, T. Y.; Sugihara, G.; Nakashima, T.; Yu, S. C. *Langmuir* **2002**, *18*, 8777-8785.
(12) Gao, J. M.; Qiao, S.; Whitesides, G. M. *J. Med. Chem.* **1995**, *38*, 2292-2301.
(13) Krishnamurthy, V. M.; Kaufman, G. K.; Urbach, A. R.; Gitlin, I.; Gudiksen, K. L.; Weibel, D. B.; Whitesides, G. M. *Chem. Rev.* **2008**, *108*, 946-1051.
(14) Bilgicer, B.; Fichera, A.; Kumar, K. *J. Am. Chem. Soc.* **2001**, *123*, 4393-4399.
(15) Lee, K. H.; Lee, H. Y.; Slutsky, M. M.; Anderson, J. T.; Marsh, E. N. G. *Biochemistry* **2004**, *43*, 16277-16284.
(16) Jackel, C.; Salwiczek, M.; Koksch, B. *Angew. Chem. Int. Ed.* **2006**, *45*, 4198-4203.
(17) Samsonov, S. A.; Salwiczek, M.; Anders, G.; Koksch, B.; Pisabarro, M. T. *J. Phys. Chem. B* **2009**, *113*, 16400-16408.
(18) Horng, J. C.; Raleigh, D. P. *J. Am. Chem. Soc.* **2003**, *125*, 9286-9287.
(19) Woll, M. G.; Hadley, E. B.; Mecozzi, S.; Gellman, S. H. *J. Am. Chem. Soc.* **2006**, *128*, 15932-15933.
(20) We also fit Eq. 5 to the data while allowing independent variation of $k_{2,0}$ in each set of data; values obtained for $k_{2,0}$ were within factors of ~2 of each other, and within factors of ~2 of the value found for $k_{2,0}$ when it was shared by each set of data (results shown in the Supplemental Information).
(21) Barluenga, J.; Trincado, M.; Rubio, E.; Gonzalez, J. M. *Angew. Chem.-Int. Edit.* **2006**, *45*, 3140-3143.
(22) Gudiksen, K. L.; Gitlin, I.; Moustakas, D. T.; Whitesides, G. M. *Biophys. J.* **2006**, *91*, 298-310.